LANGMUIR

pubs.acs.org/Langmuir Article

Molecular-Level Understanding of the Influence of Ions and Water on HMGB1 Adsorption Induced by Surface Hydroxylation of Titanium Implants

Dineli T. S. Ranathunga, Alexandra Arteaga, Claudia C. Biguetti, Danieli C. Rodrigues, and Steven O. Nielsen*

Cite This: https://doi.org/10.1021/acs.langmuir.1c01444 Read Online

ACCESS | Metrics & More | Article Recommendations | Supporting Information

ABSTRACT: Due to its excellent chemical and mechanical properties, titanium has become the material of choice for orthopedic and dental implants to promote rehabilitation via bone anchorage and osseointegration. Titanium osseointegration is partially related to its capability to form a TiO_2 surface layer and its ability to interact with key endogenous proteins immediately upon implantation, establishing the first bone−biomaterial interface. Surgical trauma caused by implantation results in the release of high-mobility group box 1 (HMGB1) protein, which is a prototypic DAMP (damage-associated molecular pattern) with multiple roles in inflammation and tissue healing. To develop different surface strategies that improve the clinical outcome of titanium-based implants by controlling their biological activity, a molecular-scale understanding of HMGB1−surface interactions is desired. Here, we use molecular dynamics (MD) computer simulations to provide direct insight into the HMGB1 interactions and the possible molecular arrangements of HMGB1 on fully hydroxylated and nonhydroxylated rutile (110) TiO_2 surfaces. The results establish that HMGB1 is most likely to be adsorbed directly onto the surface regardless of surface hydroxylation, which is undesirable because it could affect its biological activity by causing structural changes to the protein. The hydroxylated TiO_2 surface shows a greater affinity for HMGB1 than the nonhydroxylated surface. The water layer on the nonhydroxylated TiO_2 surface prevents ions and the protein from directly contacting the surface. However, it was observed that if the ionic strength increases, the total number of ions adsorbed on the two surfaces increases and the protein's direct adsorption ability decreases. These findings will help to understand the HMGB1−TiO_2 interactions upon implantation as well as the development of different surface strategies by introducing ions or ionic materials to the titanium implant surface to modulate its interactions with HMGB1 to preserve biological function.

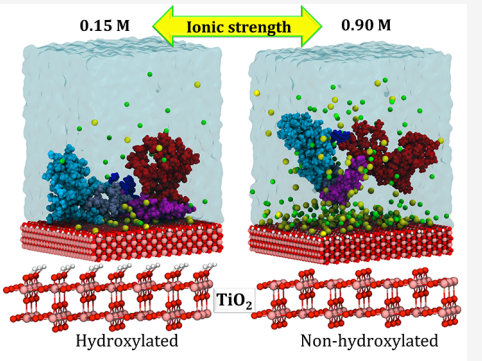

INTRODUCTION

The fundamental interactions between biomolecules and implantable inorganic materials, such as titanium, are of great interest in the fields of biomedicine, biomaterials and biochemistry. In particular, the regulation of the bioactivity of implants and how implantable biomaterials interact with host molecules is critically important. Among the biomaterials used for the development of long-term implantable medical devices, titanium has become the material of choice due to its superior chemical and mechanical properties as well as its high rate of clinical success.[1−3] Because of its relatively low density, low elastic modulus, inertness, high tensile strength, lightweight, low toxicity, high osseointegration capability, and good corrosion resistance, titanium is considered a highly biocompatible material.[4−7] Combined with low production costs, these properties have led to the widespread use of titanium in implant manufacturing.[1]

Osseointegration is an important factor in promoting implant stability. Successful titanium osseointegration is related to its surface capability to attract key endogenous proteins.[8] Indeed, titanium is currently considered as an immunomodulatory metal rather than an inert metal, partially due to the formed TiO_2 surface layer.[9−11] The physiochemical and dielectric properties, roughness, wettability, crystal structure, and composition of this oxide film on titanium implant surfaces also play a vital role in the biocompatibility and osseointegration of the implant.[12,13] This oxide layer can drive the attraction of beneficial host molecules and modulate the biological environment.[10] However, the in vivo molecular interactions with key proteins at the tissue/implant interface remain unclear, partly because of the complexity and limited methodological tools to evaluate the dynamics of titanium and

Received: May 29, 2021
Revised: July 25, 2021

host protein interactions in the biological environment upon titanium implantation.

The rupture of tissue components due to surgical trauma following implantation results in the release of damage-associated molecular patterns (DAMPs).[14,15] DAMPs are a family of endogenous intracellular or extracellular proteins that are able to trigger immune inflammatory responses upon cellular stress, tissue damage, or cell death.[14,15] High-mobility group box 1 (HMGB1) is a ubiquitous nuclear protein in the intracellular space but also acts as a prototypic DAMP molecule with important biological activities in the extracellular spaces. When released as a DAMP in the extracellular environment, HMGB1 is able to trigger inflammation and healing responses, either by itself or in combination with other molecules.[15,16] Endogenous release of HMGB1 into surgical sites has been previously shown to participate in the recruitment of inflammatory and stem cells to the injury site, thereby actively promoting healing and/or osseointegration in experimental models.[14−19] HMGB1 is also known to activate different receptors related to the innate immune response, such as Toll-like receptor 4 (TLR4) and its associated protein myeloid differentiation factor 2 (MD-2) and RAGE (receptor for advanced glycation end products).[14,15,17−19] A previous in vivo study showed that HMGB1 was present in the microenvironment surrounding titanium implants for 3 days after surgical trauma from device implantation.[15] The systemic inhibition of HMGB1, or the inhibition of its receptor RAGE, completely disrupted cellular and molecular events required for successful osseointegration.[15] Altogether, these previous findings suggest HMGB1 as a key protein involved in osseointegration of titanium implants. However, it is believed that if HMGB1 binds too strongly and irreversibly to the implant surface, it can cause structural changes to the protein and affect its biological activity.

The complete structure of HMGB1 consists of two L-shaped α-helical DNA-binding domains named A box (residues 1−79) and B box (residues 89−162), a negatively charged acidic C-terminal tail (residues 186−215), and two short linker loops, namely, 1 (residues 80−88) and 2 (residues 163−185), that connect the three segments.[17−19] The role of HMGB1 in inflammation and immunity is mainly determined by its three redox-sensitive cysteine (C23, C45, and C106) residues.[18] It is known that an isoform of HMGB1 with a disulfide bond between residues C23 and C45 and the reduced thiol form of residue C106 is required for cytokine stimulating activity.[17] This unique redox conformation of HMGB1 enables it to bind to TLR4/MD-2 complex and initiate signal transduction to induce cytokine release by macrophages.[18] It is also able to trigger RAGE in macrophages, promoting angiogenesis by a RAGE-dependent mechanism.[20] It is important to mention that macrophages play a central role in biomaterial recognition and incorporation and can further contribute to tissue healing by removing tissue debris upon injury and producing a range of growth factors, immunological molecules, and/or proteolytic enzymes for tissue remodeling.[21,22] When all three cysteines are in the fully reduced thiol form, HMGB1 will no longer activate the TLR4/MD2 or RAGE pathways but will act as a chemotactic mediator and participate in tissue repair using a different pathway.[23] The fully reduced isoform is only passively released by necrotic cells, while the disulfide isoform can be actively released by macrophages in sites of injury. Finally, because HMGB1 is a redox-sensitive molecule, the fully reduced isoform will eventually be converted to the disulfide isoform upon its release by necrotic cells in injury sites due the presence of reactive oxygen species (ROS).[24] Thus, the disulfide isoform might be the more predominant isoform in the transient phase of inflammatory response postimplantation as a result of different processes such as oxidation and active release. Therefore, to advance our understanding of HMGB1−TiO_2 surface interactions at the molecular level, the disulfide isoform of HMGB1 was chosen for this study.

In order to develop new immunomodulatory-based strategies using the constructive inflammatory effects of HMGB1 protein to improve the biological activity of titanium-based implants, a comprehensive understanding of HMGB1−TiO_2 surface interactions is necessary. Therefore, in this study we sought to understand the mechanistic details of such interactions using molecular dynamics (MD) computer simulation. MD can be considered as one of the most direct approaches to elucidate the adsorption mechanism of proteins on biomaterials and to understand the atomic details that occur at the protein−adsorbent interface.[25,26] Through MD simulations, in addition to protein−surface interactions, protein adsorption mechanisms, surface-induced conformational changes, and the effect of other factors on protein adsorption can be thoroughly investigated.[25,27−30] According to the literature, some of the factors identified as affecting the adsorption of peptides or proteins on a surface include surface chemistry,[13] pH,[31] ionic strength,[29,30] and structural topography.[32,33] The effect of all of these parameters on the adsorption of HMGB1 to the implant surface has not been systematically investigated, or only limited work has been done. Therefore, in this study, to advance our understanding of the interactions between HMGB1 and TiO_2 implant surfaces, we performed molecular dynamics computer simulations.

Since the interaction between the implant and the bone may vary depending on the implant surface characteristics (roughness, crystal structure, and composition), a variety of implant modifications have been proposed and implemented that can accelerate the osseointegration process.[13,34] In practice, the TiO_2 implant surfaces are covered with hydroxyl groups because water is easily dissociated on oxygen vacancies.[12,35] This surface hydroxylation changes the surface composition and roughness of the implant.[12,13,36,37] Fronzi and Nolan[38] reported that the adsorbed hydroxyl groups on rutile (110) can change the properties of TiO_2 nanoclusters. According to Busquim et al.,[12] the surface roughness and chemical composition can change the implant−bone interactions and hence the osseointegration capacity.[12,13,36,37]

Since surface hydroxylation affects the surface properties, it can consequently affect the interactions of molecules such as proteins with the surface.[35,39] Therefore, a comparison between unmodified (nonhydroxylated) and hydroxylated TiO_2 surfaces will provide useful information to improve our understanding of the effects of the implant surface properties on the biological activity. Hence, in this study, we used two TiO_2 surfaces, namely, an unmodified surface with no hydroxylation and a fully hydroxylated surface. Among the crystalline polymorphs of titania, rutile is a thermodynamically stable mineral in nature,[3,40,41] and the surface of rutile (110) is the most stable crystalline face.[3,40,42,43] Some results in the literature report that implants with rutile phase TiO_2 on the surface show better biocompatibility and osseointegration than those exhibiting the anatase phase.[4,12,34]

Changes in the surface properties of implants due to hydroxylation have attracted much attention from peptide/

https://doi.org/10.1021/acs.langmuir.1c01444
Langmuir XXXX, XXX, XXX−XXX

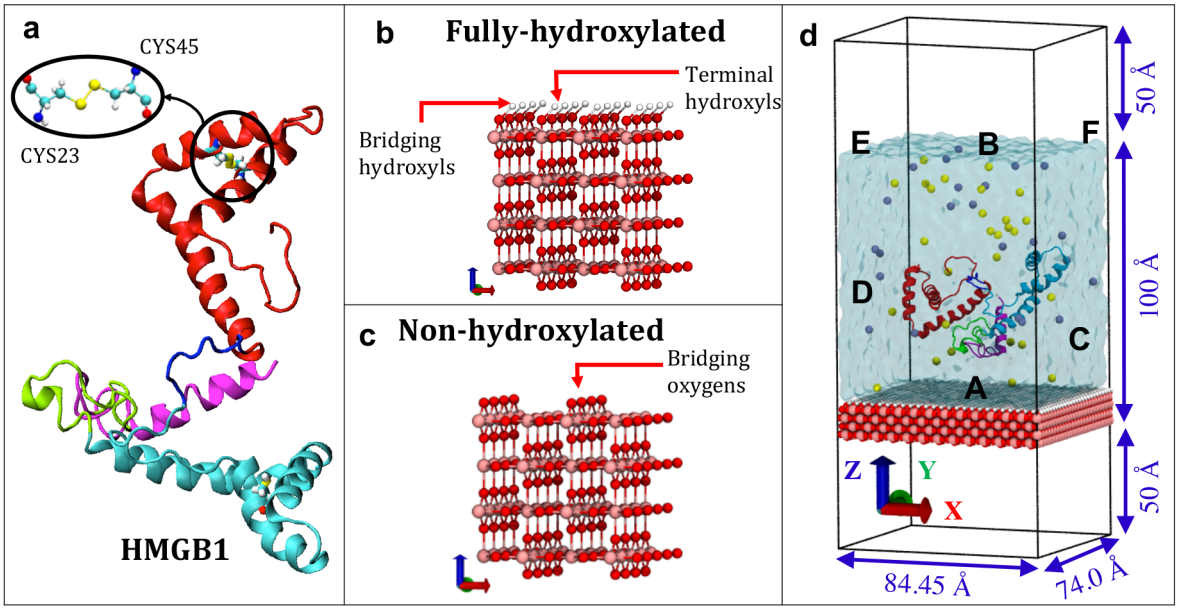

Figure 1. (a) Full-length HMGB1 structure with A box (residues 1−79) in red, B box (residues 89−162) in cyan, linker loop 1 (residues 80−88) in blue, linker loop 2 (residues 163−185) in green, and C-terminal tail (residues 186−215) in magenta. Cysteine coloring is as follows: carbon, cyan; nitrogen, blue; oxygen, red; hydrogen, white; sulfur, yellow. (b) Fully hydroxylated neutral TiO_2 surface. Here, hydrogen from water molecules combines with the bridging oxygen on the surface to form bridged hydroxyl groups, while the remaining hydroxyl groups from water molecules are attached to the 5-fold-coordinated surface Ti atoms to form terminal hydroxyl groups. (c) Nonhydroxylated neutral TiO_2 surface. Surface contains bridging oxygen atoms connected to the two underlying Ti atoms. (d) Size and initial configuration of the simulation systems. Coloring is as follows: water, light transparent blue; sodium, yellow; chloride, light purple; oxygen, red; titanium, pink; hydrogen, white. The 6 faces of the solvent box are labeled A-F.

protein adsorption investigations.[27,28,39,44] Kang et al.[27] studied the effect of TiO_2 surface hydroxylation on human serum albumin (HSA) adsorption using molecular dynamics simulations and showed that hydroxylated surfaces have strong affinity for the HSA protein compared to nonhydroxylated surfaces. Several studies in the literature report that the hydroxylation of TiO_2 surfaces can affect the behavior of not only proteins but also small molecules. Skelton and Walsh[39] performed MD simulations and studied the interaction between liquid water and rutile (110) TiO_2-modified surfaces with different amounts of hydroxylation. They showed the strong effects of surface hydroxylation on the dynamics of water at the interface. Skelton et al.[45] demonstrated how hexapeptide adsorption to rutile (110) TiO_2 is affected by the distribution of water at the interface.

Several studies in the literature reported that not only the behavior of water at the interface but also the ionic strength will affect the adsorption of amino acids and peptides on a surface.[29,46−49] The effect of solvated ions on amino acid adsorption was analyzed experimentally by comparing the adsorption isotherms generated in pure water and at different concentrations of sodium chloride by Serro et al.[50] and Vlasova and Golovkova.[51] They showed that at moderate sodium chloride concentrations, the adsorption capacity was significantly reduced, while at high concentrations, the adsorption capacity was eliminated. The experimental studies by Gao et al.[46,52] investigated the adsorption of bovine serum albumin and amino acids by mesoporous silica as a function of ionic strength and found that high salt concentrations caused a decrease in the adsorption.

Therefore, in this study, the influence of surface hydroxylation on the molecular distribution of water, ions, and HMGB1 protein at the interface was explored in detail. Previous studies have shown that when the salt concentration is high it can completely cover the surface.[28,30,46,52,53] Therefore, to extensively study the effect of ionic concentration on protein interactions, we varied the salt concentration over a wide range. The findings of this research show the influence of water and ion structuring induced by surface hydroxylation on HMGB1 adsorption, which may help in designing new strategies to enhance the biological fixation of implants.

METHODOLOGY AND SIMULATION DETAILS

Models. *HMGB1.* The HMGB1 structure consists of 215 amino acids. As shown in Figure 1, it has two DNA-binding domains, namely, the A box and B box. The A box contains residues 1−79, and the B box contains residues 89−162.[18,54] There are two linker loops (loop 1, residues 80−88, and loop 2, residues 163−185) in between these two domains and a C-terminal tail (residues 186−215).[18] Since the HMGB1 full-length model is not available, the I-TASSER online web server was used to predict the structure using the protein sequence and the available tandem HMG box domain PDB (2YRQ) structure.[17,19] The model with the highest C score was selected for the current study. In order to model the disulfide redox state of HMGB1, a disulfide bond between the C23 and the C45 cysteine residues was created. The CHARMM36 all-atom force field parameters were used to describe the protein in all of the simulations.

Surfaces. The bulk rutile structure contains 6-fold-coordinated Ti atoms and 3-fold-coordinated O atoms. In a nonhydroxylated rutile structure, the surface consists only of bridging oxygen atoms connected to the two underlying Ti atoms (Figure 1).[28,55] On a completely hydroxylated rutile surface, hydrogen from the water molecules combines with the bridging oxygen on the surface to form bridged hydroxyl

https://doi.org/10.1021/acs.langmuir.1c01444
Langmuir XXXX, XXX, XXX−XXX

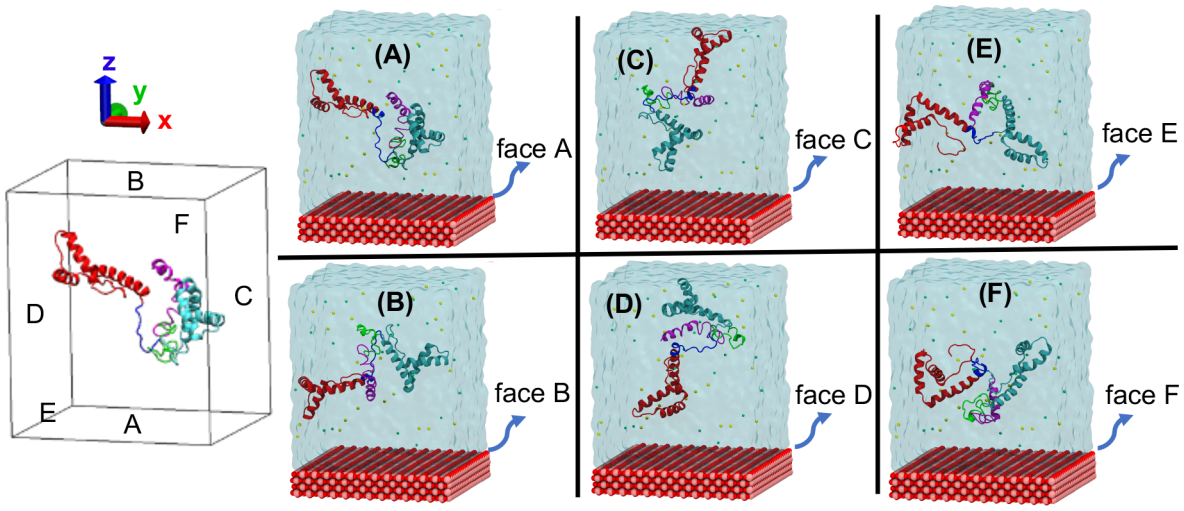

Figure 2. Six initial orientations of the HMGB1 system. Six faces of the solvated unit cell are labeled A–F. Coloring is as follows: oxygen, red; titanium, pink; hydrogen, white; sodium, yellow; chloride, green; water, light blue transparent representation. Protein is colored as follows: A box, red; linker loop 1, blue; B box, cyan; linker loop 2, lime green; C-terminal tail, magenta.

groups, while the remaining hydroxyl groups from the water molecules are attached to the 5-fold-coordinated surface Ti atoms to form terminal hydroxyl groups (Figure 1).[28] Hence, for the current study, fully hydroxylated and nonhydroxylated electrically neutral rutile (110) TiO_2 slabs were generated by changing the surface structure. First, a four-layered slab of TiO_2 with a size of 84.45 × 74.00 × 12.82 $Å^3$ in the x, y, and z directions was constructed repeating the tetragonal unit cell with a = 4.5936 Å and c = 2.9587 Å lattice constants[26,55] (Figure 1). To form a fully hydroxylated surface, hydroxyl groups were connected to the Ti atoms on the surface and the bridging oxygens were replaced by hydroxyl groups (Figure 1). The bond stretching and bending parameters were adopted from ref 56. Following Předota et al.[28] and Kang et al.,[27] the Lennard–Jones parameters of the bridging and terminal hydroxyls are kept the same as those for water. The atomic charges and the van der Waals parameters for both the nonhydroxylated and the fully hydroxylated rutile surfaces are reported in Table S1.[27,28,56] During all of the simulations, the surface groups (hydroxyl groups and bridging groups) were kept flexible while the bulk atoms were kept fixed. The total charge of the fully hydroxylated and nonhydroxylated surfaces is zero.

Simulation Details. *Protein Conformation Sampling in Water.* First, to relax the protein structure, a 5 ns long simulation of the protein immersed in water (0.15 M ionic strength) was performed (thermal equilibration data shown in Figure S11). Next, the relaxed HMGB1–water system was combined with both fully hydroxylated and nonhydroxylated TiO_2 surfaces. The HMGB1–water–TiO_2 system is composed of roughly 10^5 atoms. We considered six initial orientations of the relaxed HMGB1, which differ in their directions relative to the surface as shown in Figure 2.[26] These geometries were made by aligning the TiO_2 surface parallel to each face (labeled A–F in Figure 2) of the box consisting of HMGB1, solvating water, and 0.15 M ionic strength sodium and chloride ions (to mimic physiological conditions).[26,57,58] The TIP3P water model was used to represent water.

The protein was initially kept 15 Å above the TiO_2 surface, and the overall solvation box of 84.45 × 74.00 × 100.00 $Å^3$ was made periodic in all three directions with 50 Å of vacuum both above and below (see Figure 1d). Two repulsive walls were maintained at the water/vacuum interface and the surface/vacuum interface to prevent molecules from diffusing across the periodic boundary onto the "back" side of the titanium surface.[59] The solvated and ionized systems were first relaxed at 300 K for 100 ns under constant volume conditions (NVT), restraining the protein to its initial coordinates using harmonic constraints (k = 2 kcal/(mol·$Å^2$)).[25,60] The constraints on the protein atoms were removed gradually during the last 20 ns. A 12 Å cutoff was used for the van der Waals and short-range electrostatics interactions, while the long-range electrostatics were treated by the particle mesh Ewald technique. Thereafter, another 150 ns production run was performed for each system. All of the simulations were carried out using the NAMD software package (v.2.13)[61] and visualized using VMD.[62]

To quantify the most favorable orientation, the number of contacts, minimum distance between the protein and the surface, hydrogen-bond count (defining the hydrogen-bond distance and the angle between the donor and the acceptor as less than 3.5 Å and less than 30°, respectively[63]), and the interaction energy between the protein and the surface were calculated.[26,27] The number of contacts was measured considering the number of protein residues within 7 Å of the uppermost titanium atom layer. The minimum distance (L_M) is defined as the vertical separation distance between the uppermost titanium atom layer and the atom closest to the surface in the entire protein. The average over the final 20 ns of the trajectories was considered for the analysis. The time-averaged total nonbonded interaction energy (electrostatic + van der Waals) and energy contributions from the electrostatics and the van der Waals interactions between the protein and the TiO_2 surface were separately calculated (including the particle mesh Ewald long-range electrostatic contribution) using the NAMDenergy VMD plug-in. The most favorable orientation showing the strongest interactions with the surface was chosen for further analysis.

Effect of Ions on Protein Adsorption. In order to explain the effect of ions on the adsorption of HMGB1 to the titanium surfaces, we performed water–protein–TiO_2 simulations at different NaCl ion concentrations of 0.15, 0.30, 0.50, 0.70, and 0.90 M. The protein was first placed 15 Å above the TiO_2

https://doi.org/10.1021/acs.langmuir.1c01444
Langmuir XXXX, XXX, XXX–XXX

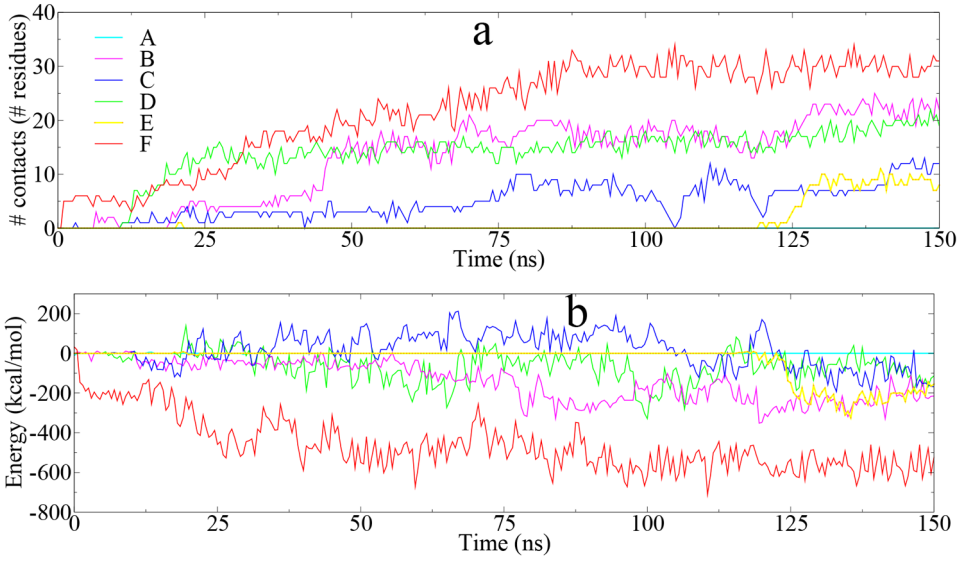

Figure 3. Results obtained for the six HMGB1 conformations on the fully hydroxylated surface. (a) Number of residues within 7 Å of the uppermost titanium atom layer vs time. (b) Interaction energy between the protein and the surface vs time.

surface and then solvated with TIP3P water to obtain a 84.45 × 74.00 × 100.00 Å^3 rectangular unit cell. The resulting system with a total charge of −5 e (the charge of HMGB1) was neutralized at different ionic strengths by adding different amounts of sodium and chloride ions. In the initial configuration ions were placed randomly and homogeneously in the water phase. The CHARMM36 force field is used to describe the water and ion parameters. Then NVT simulations at 300 K were conducted to equilibrate the system with the protein atoms restrained to their initial positions for 5 ns (k = 2 kcal/(mol·Å^2)). Then, the protein was gradually released over the next 10 ns, and the system was run for another 100 ns at 300 K. The protein adsorption to the surface was quantified using the number of contacts, minimum distance, hydrogen-bond count, and interaction energy. Since the average results (number of contacts, interaction energy, and L_M) remained the same after 100 ns in the 150 ns protein sampling simulations (for example, the average number of contacts for conformation F on the nonhydroxylated surface after 100 ns is 19 ± 2, which remained the same after 150 ns), only 100 ns long simulations were performed at different ion concentrations to save computational resources.

To quantify the orientation of the HMGB1 protein with the fully hydroxylated and nonhydroxylated TiO_2 surfaces at different ion concentrations, first the angles between the three principal axes of the protein and the TiO_2 surface normal vector (z direction) were measured considering the dot products. The principal axes of inertia of a protein are a set of eigenvectors that passes through the center of mass of the protein corresponding to the symmetry of the protein, related to the protein's mass distribution. Following Foote and Raman[64] and Harrison et al.,[65] the principal axes of the protein were calculated and are shown in Figures S12 and S13, and the angles between each principal axis and the surface normal were measured. To show the correlation between the protein orientation on the surface and the ionic concentration, heat maps were generated (Figure S14). Here, the protein orientation was represented by the angle between principal axis 3 and the surface normal vector in the z direction. The dipole moment vector angle of the protein with the surface normal was measured using the vector dot product to further quantify the orientation (shown in Figure S15).[66] To further compare how the protein adsorption varies with its orientation over time, heat maps were generated considering the distance between each protein residue and the surface during the adsorption at different ionic concentrations (Figures 10 and S16).

RESULTS AND DISCUSSION

Protein Conformational Sampling in Water. In this study, we performed MD computer simulations to obtain molecular-level understanding of the interactions of HMGB1 with titanium implants that can occur following device implantation and the onset of inflammatory and healing events. In order to study the effect of titanium surface hydroxylation on the adsorption of HMGB1, two neutral rutile (110) TiO_2 surfaces, namely, fully hydroxylated and non-hydroxylated, were prepared (Figure 1). If a protein is initially far from the surface, it will have enough time to rotate and approach the surface with a preferred orientation for adsorption. However, given the time scale limitation of MD, in order to sample this protein orientation preference, six initial scenarios are considered in which HMGB1 is initially positioned near the surface in different orientations (Figure 2).[26,27] In these initial configurations, the protein was placed above the surface with a protein−surface minimum distance of 15 Å, which is outside the van der Waals cutoff (Figure 2). Then, the most favorable protein orientations for adsorption on the two surfaces were determined for further study. To mimic physiological conditions, the aqueous systems were prepared with 0.15 M NaCl.[57,58]

During the simulations, we observed that some orientations clearly favored surface adsorption while others showed unstable adsorption including migrations along the surface and desorption with time. To quantify the adsorption of the protein to the surface, four main parameters were used:[26] the number of contacts, the interaction energy between the protein and the surface, the time taken for HMGB1 to adsorb and stabilize on the surface (with no migrations), and the minimum distance between the protein and the surface

https://doi.org/10.1021/acs.langmuir.1c01444
Langmuir XXXX, XXX, XXX−XXX

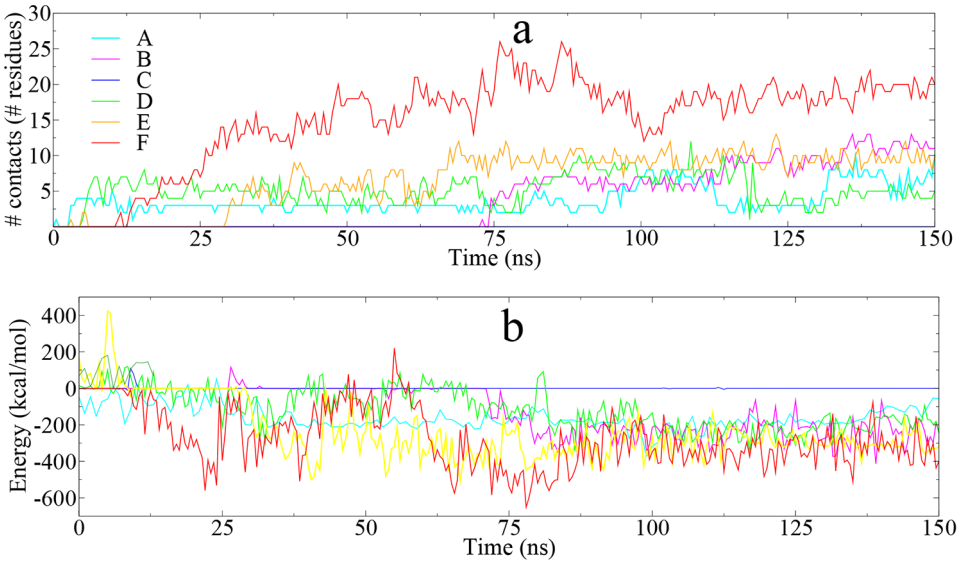

Figure 4. Results obtained for the six HMGB1 conformations on the nonhydroxylated surface. (a) Number of residues within 7 Å of the uppermost titanium atom layer vs time. (b) Interaction energy between the protein and the surface vs time.

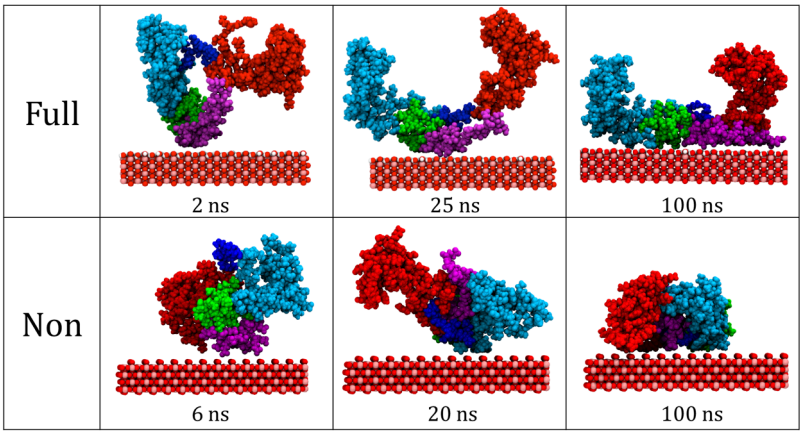

Figure 5. Time lapse images of conformation F adsorbing on fully hydroxylated and nonhydroxylated TiO_2 surfaces. Coloring as follows: A box, red; linker loops 1, blue; B box, cyan; linker loop 2, lime green; C-terminal tail, magenta; surface oxygen, red; titanium, pink; surface hydrogen, white.

(L_M). The main interacting residues were also monitored to understand the types of protein−surface interactions.

Among the six conformations of HMGB1 studied on the fully hydroxylated TiO_2 surface, conformation F exhibits the fastest surface adsorption (2 ns, Table S2). It also shows the strongest interaction energy and the largest number of contacts. The number of contacts increases over time for conformation F until the interaction energy stabilized at around 580 kcal/mol after ∼85 ns (Figure 3). The results from the different orientations (A−F) show noticeable differences. Therefore, on the time scale considered in this study, we can say that protein conformation F exhibits the strongest binding to the surface. Configurations A and E show large minimum separation distances and lower or zero contacts, indicating a weak adsorption preference to the surface compared to other orientations.

While the behavior of the six different conformations of HMGB1 on the nonhydroxylated TiO_2 surface was somewhat different from the fully hydroxylated surface, interestingly, the strongest adsorption to the surface was again observed for conformation F. Figure 4a clearly shows the highest number of contacts between conformation F and the surface, even though it is not the conformation that first binds to the surface (Figure 4 and Table S3). Although for this surface there is not an obvious difference in the interaction energies in Figure 4b, when we consider the average value over the last 20 ns, conformation F exhibits the highest average interaction energy as reported in Table S3.

The simulations clearly show orientation-dependent protein interactions. For some orientations HMGB1 does not adsorb to the TiO_2 surfaces during the considered time frame. Orientation F displays the strongest adsorption to both surfaces. Therefore, protein orientation F was selected for further analysis.

Structural Dynamics and Protein−Surface Interactions. In order to study the surface-induced adsorption behavior of the HMGB1 protein in detail, we investigated the structural dynamics of protein conformation F at the titanium implant interface. Since conformation F displays a substantially higher adsorption preference than the other five conformations

https://doi.org/10.1021/acs.langmuir.1c01444
Langmuir XXXX, XXX, XXX−XXX

on both fully hydroxylated and nonhydroxylated TiO_2 surfaces, we first examined which residues are initially close to the surface (Figure S1). In conformation F, the C-terminal tail and linker loop 2 reside close to the surface; specifically the side chains of E186, E187, E188, E189, D190, E191, E192, D193, E194, E195, D196, E197, E198, E199, E200, E201, D202, E203, E204, D205, and E208 in the C-tail and K167, D169, A170, and K185 in loop 2 point directly at the surface while some parts of box A (S53, A54, K55, and K59) lie in the vicinity of the surface (Figure S1). This is evidence for the importance of electrostatic interactions between the surface and the charged and polar residues of the protein. The initial orientation of conformation B shows some similarities to conformation F in that more of box A and some parts of the C tail point directly at the surface; hence, it shows the second strongest adsorption to both surfaces.

After 2 ns, conformation F comes within 7 Å of the fully hydroxylated surface through residues D193, E194, E200, E189, D180, and D190 in the C tail and linker loop 2 (Figures 5 and 10). These residues immediately stabilize on the surface and bring more residues from the C tail and loop 2 to the surface. After about 60 ns, some residues of box B and box A were observed to be adsorbed on the surface, causing structural changes in the protein with the C-terminal tail positioned parallel to the surface (Figure 5).

The first contacts of protein conformation F with the nonhydroxylated surface are established by the E200, E199, D193, E194, and E189 residues of the C tail (Figures 5 and S16). However, these interactions were observed to be transient, and a rotation of the protein was observed over time to increase its surface binding. About 20 ns later, interactions with residues K90 and D91 in box B initiate stable contacts, bringing the protein closer to the surface (Figure 5). Over a longer time span, some residues from box A (K7, H27, and K28) were observed to migrate and stabilize on the surface. As a result, the C tail was not observed to be aligned parallel to the surface. This shows that even though the initial protein conformation above the two surfaces was the same, different absorption patterns were observed (Figure 5) within the 150 ns time frame under consideration, indicating that the surface characteristics play a major role in protein adsorption.

Tables S2 and S3 list the main interacting residues of protein orientation F with the two titanium surfaces over the last 20 ns of the adsorption simulations. When we compare these residues, we can see that acidic residues and basic residues show high affinity for both the fully hydroxylated and the nonhydroxylated surfaces, which is in accordance with the literature.[5,26,67−70] Due to van der Waals attractions, some polar and nonpolar residues were also observed in the vicinity of the surface. To quantify this, we measured the electrostatic and van der Waals interaction energies between HMGB1 conformation F and the fully hydroxylated and nonhydroxylated surfaces in Figure 6. The results indicate that electrostatics play a major role in protein adsorption. Over the last 20 ns of the simulations, the electrostatic interaction between HMGB1 and the fully hydroxylated surface is greater than that in the nonhydroxylated system. The large fluctuations of the total and electrostatic interaction energies (Figures 4b and 6) observed in the HMGB1−nonhydroxylated TiO_2 system reveal the weaker binding of the protein on the nonhydroxylated surface. We noticed that the van der Waals interaction energy between the protein and the nonhydroxylated surface is higher than that of the fully hydroxylated surface (see Figure 6).

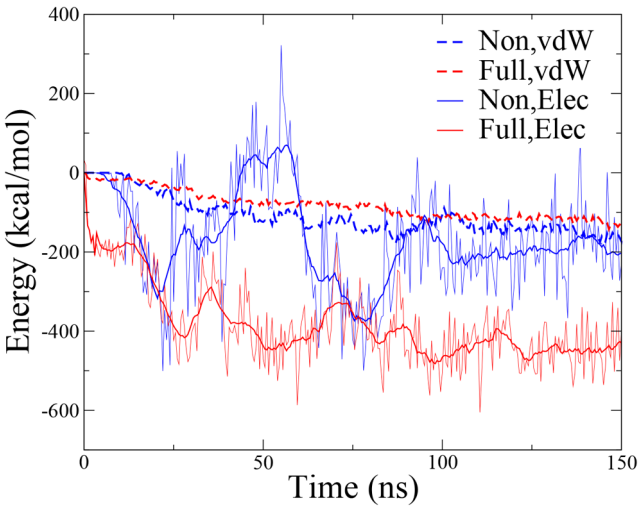

Figure 6. Electrostatic (solid lines) and van der Waals (dotted lines) interactions between HMGB1 conformation F and the fully hydroxylated (red) and nonhydroxylated (blue) surfaces. For the electrostatic interactions, a smoother trendline is also shown for clarity.

However, collectively the electrostatic and dispersion interactions cause a significant difference in the time-averaged total protein−surface interaction energies of the two systems (Tables S2 and S3). In summary (see Tables S2 and S3), we conclude that the fully hydroxylated TiO_2 surface has a greater affinity for HMGB1 compared to the nonhydroxylated TiO_2 surface. In an aqueous environment, we observed the direct binding of HMGB1 to the TiO_2 surface regardless of its hydroxylation state, which causes structural changes to the protein (Figure 7).

Structural Dynamics of Water and Hydrogen Bonds at the Interface. To further investigate the different adsorption mechanisms observed above, the behavior of water at the interface was studied. Visual inspection of the molecular dynamics trajectories revealed a well-structured layer of water molecules at the interface for both neutral titanium surfaces (Figure 7). These layers seem to affect the adsorption of protein to the surface.[5,26,67−70] Three structured water layers were clearly visible near the nonhydroxylated surface and two layers near the fully hydroxylated surface. To quantify the distribution of water at the surface, density profiles normal to the interface were constructed. Figure 8 shows the average density distribution over the last 20 ns as a function of distance from the surface. The water density profiles on the fully hydroxylated and nonhydroxylated surfaces show excellent agreement with the profiles reported in work by Skelton and Walsh[39] and Kang et al.[27] From Figure 8, the water in the interfacial region and the bulk region can be clearly distinguished by the varying density and constant density of water oxygen atoms, respectively.

The density profiles in Figure 8b for the nonhydroxylated surface show a peak corresponding to the bridging oxygens at 2.5 Å and peaks at 3.5, 5.9, and 8.7 Å for the first, second, and third water layers, respectively. These strong peaks support the more pronounced first two layers of water observed in Figure 7 (for the nonhydroxylated surface). The hydrogen density profile in Figure 8b shows a peak at 4.1 Å, following the water oxygen peak at 3.5 Å, which corresponds to the first water adlayer. This peak clearly shows the orientation of the first

https://doi.org/10.1021/acs.langmuir.1c01444
Langmuir XXXX, XXX, XXX−XXX

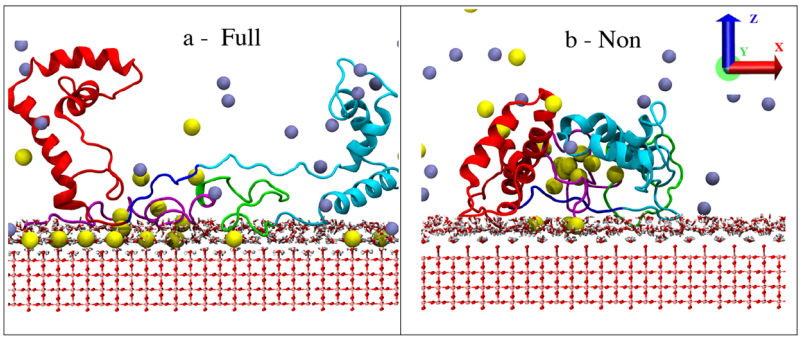

Figure 7. HMGB1 adsorption and denaturation on (a) the fully hydroxylated surface and (b) the nonhydroxylated surface. Coloring as follows: HMGB1 A box, red; linker loop 1, blue; B box, cyan; linker loop 2, lime green; C-terminal tail, magenta; oxygen, red; titanium, pink; hydrogen, white; sodium, yellow; chloride, light purple.

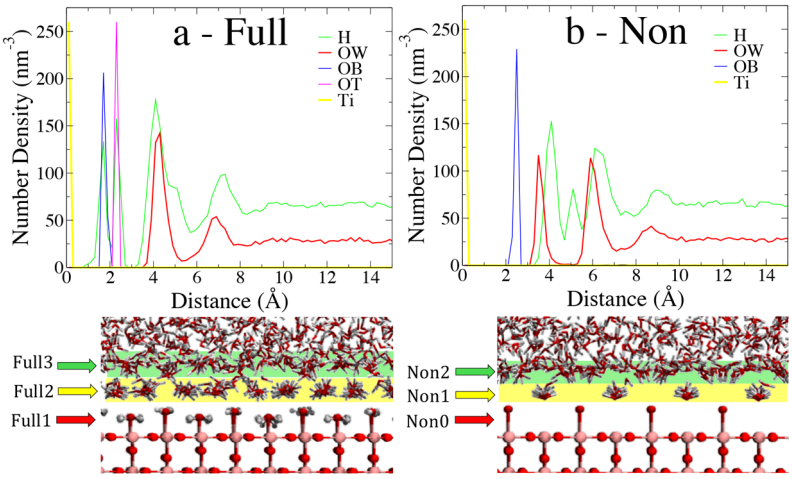

Figure 8. Average atomic density distribution of water oxygen (OW), hydrogen (H), surface bridging oxygen (OB), surface terminal oxygen (OT), and surface titanium atoms (Ti) on the (a) fully hydroxylated TiO_2 and the (b) nonhydroxylated TiO_2 surfaces as a function of the distance from the uppermost titanium atom layer. Average over the last 10 ns. Lower panel shows the different water layers observed on the surfaces and the nomenclature used in the manuscript.

layer of water, where the water molecules point their hydrogen atoms away from the titanium surface. The next two hydrogen peaks in Figure 8b at 5.1 and 6.1 Å, around the oxygen peak at 5.9 Å, show the orientation of the second water layer where only one of the water hydrogen atoms faces the bridging oxygen atoms on the surface. A similar water distribution was reported on the neutral nonhydroxylated TiO_2 surface by Skelton and Walsh,[39] who studied hexapeptide adsorption on the rutile (110) surface. We observed a water depletion region between the first and the second water layers. It is observed that no water penetrates to the surface, which is reflected by the zero overlap of the water profile with the surface.[63]

A reorientation of the water molecules was observed near the hydrophilic TiO_2 surface as a result of strong electrostatic interactions.[63] Due to the strong network of hydrogen bonds, the first layer of water on the nonhydroxylated surface is very stable and prevents other molecules from directly adsorbing onto the surface. Therefore, essentially no protein residues or ions pass beyond this first layer of water (Figure 7b). Even the molecules that transiently pass through the first water adlayer were repelled as time passed. This also explains the lower number of contacts between HMGB1 and the nonhydroxylated surface and the higher minimum distances (>4.7 Å) in Table S3.

On the fully hydroxylated surface, the density distribution show peaks at 1.7 and 2.3 Å, which correspond to bridging oxygen atoms and terminal oxygen atoms, respectively (Figure 8a). Then, an oxygen peak at 4.3 Å and a hydrogen peak at 4.1 Å show the arrangement of the first layer of water. Since the fully hydroxylated TiO_2 exclusively has hydroxyl groups on the surface, water molecules near the surface (the first adlayer) tend to orient by facing hydrogen atoms toward surface oxygen atoms and water oxygen atoms toward surface hydrogen atoms. On the other hand, the hydroxyl groups on the surface are also observed to orient to capture the approaching water molecules, thereby minimizing their energy.[63] Since the hydroxyl groups on the fully hydroxylated surface have similar parameters to the −OH groups of water, a similar gap is obtained between the surface hydroxyl peak and the first water oxygen (OW) peak in the density profile. In contrast to the nonhydroxylated system, less ordering of the second water layer was observed in the hydroxylated system, as evidenced by the peak height in Figure 8. Clear ordering and density modulations were observed up to 8 Å from the hydroxylated surface and up to 10 Å from the nonhydroxylated surface.

In order to further explore the influence of water on protein adsorption, we examined the hydrogen bonds formed at the interface before and after protein adsorption. We first performed 25 ns simulations of water/TiO_2 without a protein

https://doi.org/10.1021/acs.langmuir.1c01444
Langmuir XXXX, XXX, XXX−XXX

or ions using both the fully hydroxylated and the nonhydroxylated surfaces. To explain the results, we introduce some terminology as follows (see Figure 8). The first water adlayer on the nonhydroxylated surface is denoted as Non1, and the second water layer is denoted as Non2. On the fully hydroxylated surface, the surface −OH groups are denoted as Full1 and the first water layer as Full2.

The Non1 intralayer hydrogen-bond count fluctuates less than the other layers (among both surfaces), confirming a stable first water adlayer described in the previous section (Figure S3a and Table 1). However, the number of intralayer hydrogen bonds in the Non1 layer is lower than the number of hydrogen bonds between the Non1 and the Non2 layers. On the other hand, in the fully hydroxylated system, the Full1 layer shows more intralayer hydrogen bonds than those between Full1 and Full2, thus reducing the possibility of hydrogen-bond formation between the Full1 and the Full2 layers, which is consistent with the observations of Monti[5] and Wang et al.[71] It was also found that the number of hydrogen bonds between the Full1 and the Full2 layers on the hydroxylated surface was lower than the corresponding number (between Non1-Non2) on the nonhydroxylated surface. From Figure S3a and Table 1, it can be seen that on the nonhydroxylated surface, an average of 148 hydrogen bonds connect the Non1-Non2 layers, and an average of 98 hydrogen bonds connect the Full1−Full2 layers. The lower number of interlayer hydrogen bonds close to the fully hydroxylated surface is a major reason the protein and ions can move closer to this surface as seen in Figure 7 and results in a higher number of protein contacts as observed in Table S2.

Table 1. Average Number of Hydrogen Bonds in the Presence and Absence of Protein (Conformation F) and Ions (0.15 M Ionic Strength)

no. of H bonds	without protein and ions	with protein and ions
Full1−Full1	403 ± 21	363 ± 28
Non1−Non1	20 ± 6	23 ± 6
Full1−Full2	98 ± 9	87 ± 7
Non1−Non2	148 ± 9	147 ± 9
Full2−Full2	396 ± 21	389 ± 22
Non2−Non2	419 ± 26	359 ± 27

When we compare the nonhydroxylated data in Table 1, no significant change was observed in the presence or absence of protein, in the intralayer Non1 hydrogen-bond count, nor in the interlayer hydrogen-bond count between the Non1 and the Non2 layers. However, in the fully hydroxylated system, noticeable changes were observed in the number of hydrogen bonds with and without the protein.[27] In Figure S3b and Table 1, we observed a decreasing trend in the Full1−Full2 hydrogen-bond count and the intralayer hydrogen-bond count over time as the protein adsorbed onto the fully hydroxylated surface. This indicates that as the protein reaches the surface, the existing hydrogen-bonding network is disrupted and the possibility to form hydrogen bonds with the protein increases with time. To confirm this, we measured the number of hydrogen bonds between the protein and the water layers with time and observed an increasing trend (Figure S4). The number of hydrogen bonds between the protein and the surface, the protein and the first water adlayer, and the protein and the second water layer in the fully hydroxylated system is higher than that in the nonhydroxylated system (see Figure S4). In addition, when the protein is adsorbed, we observe a small increase in the number of water molecules in the Full2 and Non1 layers[27] (see Figure S5), which indicates that the protein brings some water molecules (that are already attached to the protein) closer to the surface. However, this will not affect the intralayer or interlayer hydrogen-bond counts in the existing layers because for the new water molecules the sites available for hydrogen-bond formation are already occupied by the protein.

Details of Protein Binding at the Surface−Water Interface. In the fully hydroxylated and nonhydroxylated systems, the side chains of some protein residues adsorb onto the surface, mediated by the interfacial water layer. Figure 7 and Table S4 show the details of the protein adsorption at the interface. On the time scale considered in this study, more residues were adsorbed on the fully hydroxylated surface compared to the nonhydroxylated surface. Charged residues were recognized as the main interacting residues in both systems compared to polar/nonpolar residues. From Figures 7a and 5, we can clearly see that on the fully hydroxylated surface, some adsorbed residues travel very close to the surface and interact with the Full1 layer (surface −OH layer), replacing the water in the Full2 layer. At the same time, other groups stay in the third water layer (Full3) region and interact with the Full2 layer. If we look at the orientation of the charged residues that travel very close to the fully hydroxylated surface in Table S4, we can see that the oxygen atoms in the $-COO^-$ groups of the ASP and GLU residues tend to form hydrogen bonds with the hydrogen atoms of the surface −OH groups. On the other hand, the hydrogen atoms in the $-NH_3^+$ group of the LYS and ARG residues form hydrogen bonds with the surface hydroxyl oxygen atoms.

As shown in Figure 7b, the protein residues on the nonhydroxylated surface do not disturb or pass through the Non1 water layer and thus maintain a certain distance from the surface. However, some residues do interact with the surface bridging oxygens. Most of the adsorbed residues are located in the Non2−Non3 region. In Table S4 we can see that the ASP and GLU residues have their $-COO^-$ group oxygen atoms interacting with the hydrogen atoms in the Non1 water layer. Conversely, in the LYS and ARG residues, the hydrogen atoms in $-NH_3^+$ form hydrogen bonds with the surface bridging oxygens (Non0 layer) and water oxygens in the Non1 layer.

The separation standard deviation of all of the residues listed on the fully hydroxylated surface in Table S4 is less than the separation standard deviation on the nonhydroxylated surface, which indicates that the protein is more stable on the hydroxylated surface than on the nonhydroxylated surface. On the nonhydroxylated surface, we also observed that some of the residues (for example, for D213 L_M = 4.66 Å and for K87 L_M = 4.66 Å) that traveled much closer to the surface during the simulation were transient and did not remain on the surface. As shown in Table S4, for acidic residues such as ASP and GLU, in both systems, atoms traveling to the vicinity of the surface are oxygen atoms in the $-COO^-$ group. On the other hand, among the basic residues, it is mainly $-NH_3^+$ hydrogen atoms that approach the surface.[27,39,72] When considering the average distance (L_M) over the last 10 ns reported in Table S4 for the charged residues absorbed on the fully hydroxylated surface, we can see that LYS (a basic residue) gets closest to the surface. On the other hand, in the nonhydroxylated case, ASP (an acidic residue) approaches closest to the surface.

https://doi.org/10.1021/acs.langmuir.1c01444
Langmuir XXXX, XXX, XXX−XXX

Effect of Ions on Protein Adsorption. In the previous section, we discussed the effect of interfacial water molecules on protein absorption on the two neutral TiO_2 surfaces. When examining the molecular behavior at the interface, we observed that in addition to water, ions also showed some influence on protein adsorption. Therefore, to study the role of ions on protein adsorption, we performed HMGB1−water−TiO_2 simulations at different sodium chloride (NaCl) salt concentrations of 0.15, 0.30, 0.50, 0.70, and 0.90 M on both the nonhydroxylated and the fully hydroxylated TiO_2 surfaces. HMGB1 conformation F was used as the initial protein configuration for these simulations. Figures S6 and S7 show the ion distribution of each system on the fully hydroxylated and nonhydroxylated surfaces after protein adsorption (after 100 ns).

For the fully hydroxylated TiO_2 interface, the ions are strongly adsorbed onto the surface due to their electrostatic interactions. When the ionic strength of the medium increases, the number of ions adsorbed on the fully hydroxylated surface also increases (Figure 9). Interestingly, as the ion concentration increases, the ions tend to form a double-layered structure on the surface (Figure S6).[28,73] Sodium ions form the first monolayer on the surface, and chloride ions form a second layer. Figure S8 shows the average density distribution of cations and anions over the last 10 ns as a function of distance from the surface.

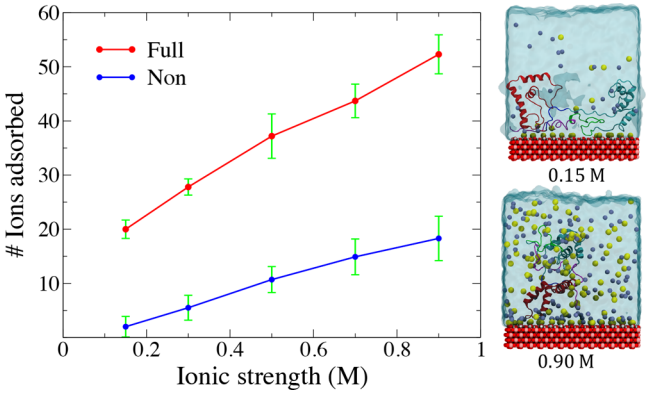

Figure 9. Total number of ions adsorbed (within 7 Å) on the fully hydroxylated and nonhydroxylated surfaces vs ionic strength. Snapshots of HMGB1 conformation F adsorption on the fully hydroxylated surface in water at 0.15 and 0.90 M ionic strengths.

The cation distribution on the fully hydroxylated surface in Figure S8 shows a sharp peak indicating a structured layer adsorbed on the surface. The anion peaks are broad and located above the cation layer, thus forming a double layer. The heights of the peaks indicate that the degree of adsorption and ordering of anions is a factor of 6 lower than that of cations on the fully hydroxylated surface.

On the other hand, the cation and anion layering on the nonhydroxylated surface is not as prominent as on the fully hydroxylated surface (Figures S6−S8). Compared with the fully hydroxylated systems, the peak heights for the nonhydroxylated system are a factor of 3 lower. Still, as the ionic strength increases, more ion adsorption occurred (Figure 9). Interestingly, the ions failed to penetrate the first water adlayer for the same reason as that explained in the previous section. From the simulation trajectory snapshots in Figure S7 and the density distribution curve in Figure S8, a randomly distributed mixture of cations and anions is observed in the vicinity of the surface without forming a clear double layer as was seen on the fully hydroxylated surface.

On both the fully hydroxylated and the nonhydroxylated surfaces, the peak heights of the sodium and chloride ions increase with increasing ionic strength (Figure S8). Therefore, as seen in Figure 9, as the ionic strength increases, the total number of ions absorbed on the surfaces also increases. The increase in the amount of ions adsorbed on the fully hydroxylated surface is greater than that on the nonhydroxylated surface. Moreover, the adsorbed ions on both surfaces tend to shield the protein from directly binding to the surface. Therefore, as the ionic strength increases, less protein adsorption occurs (see Figures S6 and S7).

To understand the mechanism of protein adsorption at different ionic concentrations, we measured the number of contacts, the minimum distance between the protein and the surface, and the interaction energy between the protein and the surface. Time-dependent traces of these quantities are shown in Figures S9 and S10. From Figure S9 we can see a significant decrease in the number of contacts and in the interaction energy when the ionic concentration increases from 0.15 to 0.90 M. From the results in Table 2, we can rank the protein adsorption extent under different ion concentrations on the fully hydroxylated surface as 0.15 > 0.30 > 0.50 > 0.70 > 0.90 M.

This shows that when the ion concentration increases, the adsorption capacity of the protein on the surface decreases. As previously observed, at high ion concentration more ions are adsorbed on the surface and tend to shield the protein from

Table 2. Time-Averaged Results of HMGB1 Conformation F on the Fully Hydroxylated TiO_2 Surface at Different Ionic Concentrations[a]

ionic strength (M)	time taken to adsorb (ns)	no. of contacts (no. of residues)	energy (kcal/mol)	L_M (Å)	main interacting residues
0.15	2	31 ± 2	−577.7 ± 60.6	3.9 ± 0.2	A160, A164, R163, D169, D190, D193, D205, D211, D212, D213, D214, E189, E194, E195, E199, E200, E201, E206, E209, E210, E215, I159, K157, K165, K167, K76, P168, P80, T77, Y162, Y78
0.30	14	14 ± 1	−479.7 ± 50.2	4.2 ± 0.3	D190, D196, D214, E191, E192, E195, E197, E200, E201, E204, E215, K184, K29, K30
0.50	11	10 ± 1	−438.4 ± 49.5	4.6 ± 0.3	D193, D196, E191, E192, E195, E197, E198, E199, E200, E201
0.70	12	8 ± 1	−342.7 ± 43.9	4.7 ± 0.2	D190, D193, E189, E192, E194, E195, E199, E200
0.90	62	6 ± 1	−13.9 ± 37.5	4.7 ± 0.3	D33, H31, K28, K29, K30, P32

[a]Average over the last 20 ns (from the 100 ns adsorption simulation). The amino acids are represented by their single-letter abbreviations. The results of HMGB1 conformation F on the nonhydroxylated surface at different ionic concentrations are given in Table S5.

https://doi.org/10.1021/acs.langmuir.1c01444
Langmuir XXXX, XXX, XXX−XXX

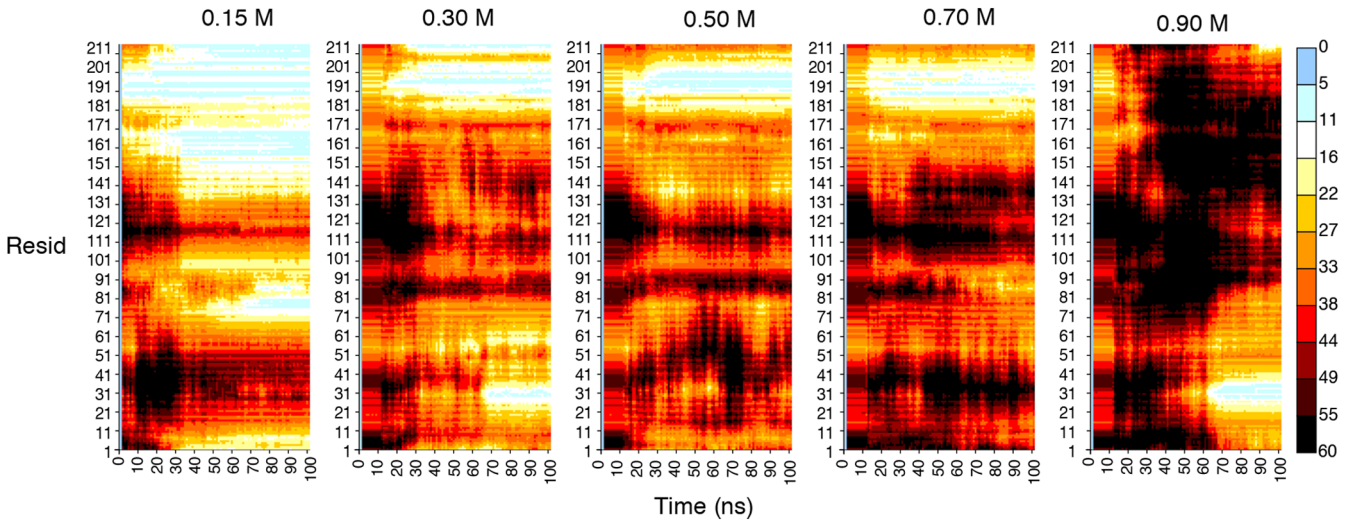

Figure 10. Heat map showing the distance between each residue of the HMGB1 protein and the fully hydroxylated surface with time at different ionic strengths. Color scale bar shows the residue−surface distance in Angstroms. Distance is measured as the z distance from the uppermost titanium atom layer to the center of mass of the residue. Results of the nonhydroxylated systems are shown in Figure S16.

direct binding. In general, small ions and water molecules compete with proteins to adsorb to the surface.[68] Since they can diffuse faster than large protein molecules, water and ions will adsorb and structure on the surface before the protein can reach the surface. This can block the protein from adsorbing. From Figure S9b we can see the proximity of the protein to the surface in the presence of ions. It is clear that as the ion concentration increases, the time required for protein adsorption increases (Figure S9b). At an ionic concentration of 0.15 M the protein reaches the surface within 2 ns, whereas at an ionic concentration of 0.90 M the protein takes about 62 ns to stabilize on the fully hydroxylated surface (Table 2) and even then is farther from the surface compared to the lower ionic strength cases (Figure S9b).

A similar protein behavior was observed for the nonhydroxylated systems with increasing ionic concentration (Figure S10). However, the differences with ionic strength in the number of contacts and the interaction energy are not as pronounced as in the fully hydroxylated case (Figure S10). Tables 2 and S5 show the minimum distance reached between the protein and the fully hydroxylated and the nonhydroxylated surfaces in different ionic environments. The minimum distances are higher for the nonhydroxylated systems compared to the fully hydroxylated systems. This is because the first water adlayer on the nonhydroxylated surface can repel ions and protein residues so that they cannot directly adsorb to the surface. Tables 2 and S5 report the amino acids closest the surface in each case.

To quantify the orientation of the HMGB1 protein with the fully hydroxylated and nonhydroxylated surfaces at different ionic concentrations, the angles between the three principal axes of the protein and the TiO_2 surface normal vector (z direction) were measured. Figures S12 and S13 show the final simulation snapshots with the three principal axes of the protein in each system at different ionic concentrations. On both the fully hydroxylated and the nonhydroxylated surfaces, the results revealed that the angle between principal axis 3 (symmetry axis) of the protein and the surface normal vector (in Table S6, angle 3-Z of both surfaces) decreases with increasing ionic concentration (see Table S6, Figures S12 and S13). This suggests that at lower ionic concentrations the protein tends to orient parallel to the surface due to the protein's ability to form more contacts with the surface. Hence, more collapsed and denatured protein orientations were observed at lower ionic concentrations. To clearly show this correlation between the protein's orientation on the surface and the ionic concentration, heat maps were generated considering the orientational changes of the protein with time (Figure S14). From Figure S14 it is observed that in both the fully hydroxylated and the nonhydroxylated systems when the ion concentration decreases the protein (principal axis 3 angle with the surface normal) adopts a more parallel orientation to the surface.

Next, the dipole vector angle of the protein with the surface normal was measured to further quantify the orientations. However, no useful relationship between this dipole angle at different ionic strengths was observed (Figure S15). The heat maps in Figures 10 and S16 show the distance between each protein residue and the surface during the adsorption at each ionic strength. The results reveal which regions of the protein interact the most with the fully hydroxylated surface compared to the nonhydroxylated surface and which regions reach the closest to those surfaces over time, affecting the orientation of the protein at different ionic concentrations (Figures 10 and S16).

The overall results show that as the ion concentration of the medium increases, the protein direct adsorption ability on the surface decreases and the protein tends to orient less parallel to the surface.

Clinical Implication and Future Directions. Immunomodulation has recently been studied as an emerging approach to adjust inflammatory events caused by implant placement to improve osseointegration and repair.[9] By making appropriate modifications to the implant surface, it is possible to regulate inflammatory responses in order to accelerate the osseointegration.[74] To develop new surface strategies, one can try to take advantage of the beneficial modulatory effects of host molecules on healing response such as HMGB1.

HMGB1 has been proposed as an essential component at the implant−protein layer to drive early implant osseointegra-

https://doi.org/10.1021/acs.langmuir.1c01444
Langmuir XXXX, XXX, XXX−XXX

tion in homeostatic conditions.[15] Therefore, knowledge of the HMGB1−implant interaction will be very useful to develop new immunomodulatory strategies to treat patients with greater susceptibility to early implant failures due to underlying conditions (e.g., a defective immune response associated with diabetes). However, when developing surface modification strategies for modulation of key proteins or soluble mediators on implant surfaces, the structural stability of the protein and its accessibility to cell receptors are important factors to consider. As we studied the behavior of HMGB1 on titanium surfaces in water, we observed that a direct and irreversible binding of HMGB1 to the TiO_2 surface can cause partial denaturation of the protein which can affect its biological functions. Therefore, a compromise between stable adsorption of the inflammatory mediator and maintenance of its activity is crucial when developing immunomodulatory surface approaches. The observed behavior of HMGB1 with increasing ionic strength should be of great interest toward future design strategies to avoid the direct adsorption of host proteins to the surface, thereby preserving their biological properties.

CONCLUSIONS

In summary, we performed MD computer simulations to understand the HMGB1 protein interactions with rutile (110) TiO_2 implant surfaces affected by surface hydroxylation using a neutral fully hydroxylated and a neutral nonhydroxylated TiO_2 surface. The simulation results indicate that under aqueous 0.15 M ionic strength conditions, HMGB1 is most likely to be adsorbed on the surface regardless of surface hydroxylation, which can cause partial denaturation of the protein and affect its biological functions. Particular orientations of HMGB1 showed preferential adsorption; among the six HMGB1 conformations we studied, conformation F, which initially points most of the charged residues directly at the surface, showed the strongest adsorption on both surfaces. However, the absorption mechanism of this HMGB1 conformation was observed to be different on the two different surfaces, illustrating the effect of surface interactions on protein adsorption. On both surfaces, the electrostatic protein−surface interactions are found to play a major role in protein adsorption compared to van der Waals interactions. The fully hydroxylated TiO_2 surface shows a greater affinity for HMGB1 than the nonhydroxylated TiO_2 surface. Moreover, surface-induced protein structural changes were observed, which may affect the HMGB1 receptor binding pathways. On both surfaces, charged residues are considered to be the main interacting residues that can first bind to the surface. The oxygen atoms of the $-COO^-$ groups in acidic residues and the hydrogen atoms in the $-NH_3^+$ groups of basic residues were observed to be in close proximity to the surfaces. On the fully hydroxylated surface, basic residues such as LYS can get closer to the surface than acidic residues, while on the nonhydroxylated surface, acidic residues such as ASP move closer to the surface.

The protein adsorption mechanisms on the two TiO_2 surfaces are observed to be affected mainly by the structure of the water molecules and ions at the interface. Due to strong electrostatic interactions, well-structured layers of water molecules were observed near the TiO_2 surfaces that influence the adsorption behavior of the protein. Due to the strong network of inter- and intralayer hydrogen bonding, a very stable first water adlayer forms on the nonhydroxylated surface which prevents other molecules from directly adsorbing onto the surface. In contrast, for the fully hydroxylated system, proteins and ions can penetrate the first water adlayer and reach the surface by disrupting the existing hydrogen-bond network. On the fully hydroxylated TiO_2 surface, the ions are strongly adsorbed to the surface due to electrostatic interactions and are positioned very close to the surface compared to the nonhydroxylated case. As the ion concentration increases, the ions on the fully hydroxylated surface tend to form a double-layer structure with excess cations adjacent to the surface. On the other hand, the layering of cations and anions on the nonhydroxylated surface is not as prominent. As the ionic strength increases, the total number of ions absorbed on both surfaces increases. The increase in the number of ions adsorbed on the fully hydroxylated surface is higher than that on the nonhydroxylated surface. Since small ions and water molecules diffuse faster than large protein molecules, they will adsorb and structure on the surface before the protein can adsorb and can prevent HMGB1 from binding to the TiO_2 surface. We rank the protein adsorption capacity under different ion concentrations on both surfaces as 0.15 > 0.30 > 0.50 > 0.70 > 0.90 M, which is to say that when the ion concentration increases, the protein adsorption capacity on the surface decreases and the protein tends to orient less parallel to the surface. Finally, considering the results of the current study, it is believed that the time frame considered is sufficient to determine the protein adsorption behavior on the titanium implant surfaces. These findings indicate that there is a huge potential for introducing ions or ionic materials to the surface to modulate the HMGB1−surface interactions and to prevent the protein's direct adsorption to the surface and structural changes that may affect its activity. We believe that these findings will encourage the development of challenging and important bioimplant materials, protein delivery techniques, and surface technologies in the future.

ASSOCIATED CONTENT

Supporting Information

The Supporting Information is available free of charge at https://pubs.acs.org/doi/10.1021/acs.langmuir.1c01444.

Force field parameters of the TiO_2 surfaces, additional simulation data of the protein conformational sampling study, supplementary figures of structural dynamics of water and hydrogen bonds at the interface, additional simulation results of the effect of ions on protein adsorption study, and results of the protein orientation analysis (PDF)

AUTHOR INFORMATION

Corresponding Author

Steven O. Nielsen − *Department of Chemistry and Biochemistry, The University of Texas at Dallas, Richardson, Texas 75080, United States;* orcid.org/0000-0003-3390-3313; Email: steven.nielsen@utdallas.edu

Authors

Dineli T. S. Ranathunga − *Department of Chemistry and Biochemistry, The University of Texas at Dallas, Richardson, Texas 75080, United States;* orcid.org/0000-0002-7860-722X

Alexandra Arteaga − *Department of Bioengineering, The University of Texas at Dallas, Richardson, Texas 75080, United States*

https://doi.org/10.1021/acs.langmuir.1c01444
Langmuir XXXX, XXX, XXX−XXX

Claudia C. Biguetti − *Department of Bioengineering, The University of Texas at Dallas, Richardson, Texas 75080, United States*

Danieli C. Rodrigues − *Department of Bioengineering, The University of Texas at Dallas, Richardson, Texas 75080, United States;* orcid.org/0000-0002-0389-0833

Complete contact information is available at: https://pubs.acs.org/10.1021/acs.langmuir.1c01444

Notes

The authors declare no competing financial interest.

■ ACKNOWLEDGMENTS

This work was supported by the University of Texas at Dallas Office of Research Seed Grant, Collaborative Biomedical Research Award (CoBRA).

■ REFERENCES

(1) Wilson, C. J.; Clegg, R. E.; Leavesley, D. I.; Pearcy, M. J. Mediation of Biomaterialell Interactions by Adsorbed Proteins: A Review. *Tissue Eng.* **2005**, *11*, 1−18.

(2) Menard, A.; Drobne, D.; Jemec, A. Ecotoxicity of nanosized TiO2. Review of in vivo data. *Environ. Pollut.* **2011**, *159*, 677−684.

(3) Diebold, U. The surface science of titanium dioxide. *Surf. Sci. Rep.* **2003**, *48*, 53−229.

(4) Tsou, H.-k.; Chi, M.-h.; Hung, Y.-w.; Chung, C.-j.; He, J.-l. In Vivo Osseointegration Performance of Titanium Dioxide Coating Modified Polyetheretherketone Using Arc Ion Plating for Spinal Implant Application. *BioMed Res. Int.* **2015**, *2015*, 1−9.

(5) Monti, S. RAD16II β-sheet filaments onto titanium dioxide: Dynamics and adsorption properties. *J. Phys. Chem. C* **2007**, *111*, 16962−16973.

(6) Fei Yin, Z.; Wu, L.; Gui Yang, H.; Hua Su, Y. Recent progress in biomedical applications of titanium dioxide. *Phys. Chem. Chem. Phys.* **2013**, *15*, 4844.

(7) Wu, C.; Chen, M.; Guo, C.; Zhao, X.; Yuan, C. Peptide-TiO2 interaction in aqueous solution: Conformational dynamics of RGD using different water models. *J. Phys. Chem. B* **2010**, *114*, 4692−4701.

(8) Martínez-Ibáñez, M.; Murthy, N. S.; Mao, Y.; Suay, J.; Gurruchaga, M.; Goñi, I.; Kohn, J. Enhancement of plasma protein adsorption and osteogenesis of hMSCs by functionalized siloxane coatings for titanium implants. *J. Biomed. Mater. Res., Part B* **2018**, *106*, 1138−1147.

(9) Vishwakarma, A.; Bhise, N. S.; Evangelista, M. B.; Rouwkema, J.; Dokmeci, M. R.; Ghaemmaghami, A. M.; Vrana, N. E.; Khademhosseini, A. Engineering Immunomodulatory Biomaterials To Tune the Inflammatory Response. *Trends Biotechnol.* **2016**, *34*, 470−482.

(10) Othman, Z.; Cillero Pastor, B.; van Rijt, S.; Habibovic, P. Understanding interactions between biomaterials and biological systems using proteomics. *Biomaterials* **2018**, *167*, 191−204.

(11) Gindri, I. M.; Siddiqui, D. A.; Frizzo, C. P.; Martins, M. A.; Rodrigues, D. C. Ionic Liquid Coatings for Titanium Surfaces: Effect of IL Structure on Coating Profile. *ACS Appl. Mater. Interfaces* **2015**, *7*, 27421−27431.

(12) Busquim, T. D. P.; Elias, C. N.; May, J. E.; Kuri, S. E.; Nascente, P. A. D. P. Titanium oxide layer on the surface of anodized dental implants. *Medical Device Materials V-Proceedings of the Materials and Processes for Medical Devices Conference*, Minneapolis, MN, USA, Aug 10−12, 2009; Gilbert, J., Ed.; ASM International, 2010; Vol. *1*, pp 60−65.

(13) Martin, J.; Schwartz, Z.; Hummert, T.; Schraub, D.; Simpson, J.; Lankford, J.; Dean, D.; Cochran, D.; Boyan, B. Effect of titanium surface roughness on proliferation, differentiation, and protein synthesis of human osteoblast-like cells (MG63). *J. Biomed. Mater. Res.* **1995**, *29* (3), 389−401.

(14) Roh, J. S.; Sohn, D. H. Damage-Associated Molecular Patterns in Inflammatory Diseases. *Immune Network* **2018**, *18*, e27.

(15) Biguetti, C. C.; Cavalla, F.; Silveira, E. V.; Tabanez, A. P.; Francisconi, C. F.; Taga, R.; Campanelli, A. P.; Trombone, A. P. F.; Rodrigues, D. C.; Garlet, G. P. HGMB1 and RAGE as Essential Components of Ti Osseointegration Process in Mice. *Front. Immunol.* **2019**, *10*, 709.

(16) Lee, G.; Espirito Santo, A. I.; Zwingenberger, S.; Cai, L.; Vogl, T.; Feldmann, M.; Horwood, N. J.; Chan, J. K.; Nanchahal, J. Fully reduced HMGB1 accelerates the regeneration of multiple tissues by transitioning stem cells to GAlert. *Proc. Natl. Acad. Sci. U. S. A.* **2018**, *115*, E4463−E4472.

(17) Panneerselvam, S.; Durai, P.; Yesudhas, D.; Achek, A.; Kwon, H. K.; Choi, S. Cysteine redox state plays a key role in the inter-domain movements of HMGB1: A molecular dynamics simulation study. *RSC Adv.* **2016**, *6*, 100804−100819.

(18) Yang, H.; Antoine, D. J.; Andersson, U.; Tracey, K. J. The many faces of HMGB1: molecular structure-functional activity in inflammation, apoptosis, and chemotaxis. *J. Leukocyte Biol.* **2013**, *93*, 865−873.

(19) Sun, S.; He, M.; VanPatten, S.; Al-Abed, Y. Mechanistic insights into high mobility group box-1 (HMGb1)-induced Toll-like receptor 4 (TLR4) dimer formation. *J. Biomol. Struct. Dyn.* **2019**, *37*, 3721−3730.

(20) Rojas, A.; Delgado-López, F.; Perez-Castro, R.; Gonzalez, I.; Romero, J.; Rojas, I.; Araya, P.; Añazco, C.; Morales, E.; Llanos, J. HMGB1 enhances the protumoral activities of M2 macrophages by a RAGE-dependent mechanism. *Tumor Biol.* **2016**, *37*, 3321−3329.

(21) Kokkola, R.; Andersson, Å.; Mullins, G.; Östberg, T.; Treutiger, C. J.; Arnold, B.; Nawroth, P.; Andersson, U.; Harris, R. A.; Harris, H. E. RAGE is the major receptor for the proinflammatory activity of HMGB1 in rodent macrophages. *Scand. J. Immunol.* **2005**, *61*, 1−9.

(22) Murray, P. J.; et al. Macrophage Activation and Polarization: Nomenclature and Experimental Guidelines. *Immunity* **2014**, *41*, 14−20.

(23) Schiraldi, M.; et al. HMGB1 promotes recruitment of inflammatory cells to damaged tissues by forming a complex with CXCL12 and signaling via CXCR4. *J. Exp. Med.* **2012**, *209*, 551−563.

(24) Kwak, M. S.; Kim, H. S.; Lee, B.; Kim, Y. H.; Son, M.; Shin, J. S. Immunological Significance of HMGB1 Post-Translational Modification and Redox Biology. *Front. Immunol.* **2020**, *11*, 1189.

(25) Ganazzoli, F.; Raffaini, G. Computer simulation of polypeptide adsorption on model biomaterials. *Phys. Chem. Chem. Phys.* **2005**, *7*, 3651−3663.

(26) Utesch, T.; Daminelli, G.; Mroginski, M. A. Molecular dynamics simulations of the adsorption of bone morphogenetic protein-2 on surfaces with medical relevance. *Langmuir* **2011**, *27*, 13144−13153.

(27) Kang, Y.; Li, X.; Tu, Y.; Wang, Q.; Ågren, H. On the mechanism of protein adsorption onto hydroxylated and non-hydroxylated TiO2 surfaces. *J. Phys. Chem. C* **2010**, *114*, 14496−14502.

(28) Předota, M.; Bandura, A. V.; Cummings, P. T.; Kubicki, J. D.; Wesolowski, D. J.; Chialvo, A. A.; Machesky, M. L. Electric double layer at the rutile (110) surface. 1. Structure of surfaces and interfacial water from molecular dynamics by use of ab initio potentials. *J. Phys. Chem. B* **2004**, *108*, 12049−12060.

(29) Wu, C.; Skelton, A. A.; Chen, M.; Vlček, L.; Cummings, P. T. Modeling the interaction between integrin-binding peptide (RGD) and rutile surface: The effect of cation mediation on Asp adsorption. *Langmuir* **2012**, *28*, 2799−2811.

(30) Sebben, D.; Pendleton, P. Analysis of ionic strength effects on the adsorption of simple amino acids. *J. Colloid Interface Sci.* **2015**, *443*, 153−161.

(31) Hug, S. J.; Bahnemann, D. Infrared spectra of oxalate, malonate and succinate adsorbed on the aqueous surface of rutile, anatase and lepidocrocite measured with in situ ATR-FTIR. *J. Electron Spectrosc. Relat. Phenom.* **2006**, *150*, 208−219.

(32) Melis, C.; Mattoni, A.; Colombo, L. Atomistic investigation of Poly(3-hexylthiophene) adhesion on nanostructured titania. *J. Phys. Chem. C* **2010**, *114*, 3401−3406.
(33) Chen, M.; Zheng, T.; Wu, C.; Xing, C. Molecular dynamics simulations of collagen adsorption onto grooved rutile surface: The effects of groove width. *Colloids Surf., B* **2014**, *121*, 150−157.
(34) Sul, Y. The significance of the surface properties of oxidized titanium to the bone response: special emphasis on potential biochemical bonding of oxidized titanium implant. *Biomaterials* **2003**, *24* (22), 3893−907.
(35) Zhang, D.; Yang, M.; Dong, S. Hydroxylation of the rutile TiO2(110) surface enhancing its reducing power for photocatalysis. *J. Phys. Chem. C* **2015**, *119*, 1451−1456.
(36) Kieswetter, K.; Schwartz, Z.; Hummert, T. W.; Cochran, D. L.; Simpson, J.; Dean, D. D.; Boyan, B. D. Surface roughness modulates the local production of growth factors and cytokines by osteoblast-like MG-63 cells. *J. Biomed. Mater. Res.* **1996**, *32*, 55−63.
(37) Lee, R. S.; Hamlet, S. M.; Ivanovski, S. The influence of titanium surface characteristics on macrophage phenotype polarization during osseous healing in type I diabetic rats: a pilot study. *Clinical Oral Implants Research* **2017**, *28*, e159−e168.
(38) Fronzi, M.; Nolan, M. Surface modification of perfect and hydroxylated TiO2 rutile (110) and anatase (101) with chromium oxide nanoclusters. *ACS Omega* **2017**, *2*, 6795−6808.
(39) Skelton, A. A.; Walsh, T. R. Interaction of liquid water with the rutile TiO 2 (110) surface. *Mol. Simul.* **2007**, *33*, 379−389.
(40) Liu, L.; Li, S.; Cao, Z.; Peng, Y.; Li, G.; Yan, T.; Gao, X. P. Well-ordered structure at ionic liquid/rutile (110) interface. *J. Phys. Chem. C* **2007**, *111*, 12161−12164.
(41) Nakamura, R.; Ohashi, N.; Imanishi, A.; Osawa, T.; Matsumoto, Y.; Koinuma, H.; Nakato, Y. Crystal-face dependences of surface band edges and hole reactivity, revealed by preparation of essentially atomically smooth and stable (110) and (100) n-TiO2 (rutile) surfaces. *J. Phys. Chem. B* **2005**, *109*, 1648−1651.
(42) Uetsuka, H.; Sasahara, A.; Onishi, H. Topography of the Rutile TiO 2 (110) Surface Exposed to Water and Organic Solvents. *Langmuir* **2004**, *20*, 4782−4783.
(43) Zhang, Y.; Bataillon-Linez, P.; Huang, P.; Zhao, Y.; Han, Y.; Traisnel, M.; Xu, K.; Hildebrand, H. Surface analyses of micro-arc oxidized and hydrothermally treated titanium and effect on osteoblast behavior. *J. Biomed. Mater. Res.* **2004**, *68A* (2), 383−391.
(44) De Stefano, C.; Foti, C.; Gianguzza, A.; Sammartano, S. The interaction of amino acids with the major constituents of natural waters at different ionic strengths. *Mar. Chem.* **2000**, *72*, 61−76.
(45) Skelton, A. A.; Liang, T.; Walsh, T. R. Interplay of sequence, conformation, and binding at the peptide?titania interface as mediated by water. *ACS Appl. Mater. Interfaces* **2009**, *1*, 1482−1491.
(46) Gao, D.; Lin, D. Q.; Yao, S. J. Mechanistic analysis on the effects of salt concentration and pH on protein adsorption onto a mixed-mode adsorbent with cation ligand. *J. Chromatogr. B: Anal. Technol. Biomed. Life Sci.* **2007**, *859*, 16−23.
(47) Hamad, S.; Sánchez-Valencia, J. R.; Barranco, A.; Mejías, J. A.; González-Elipe, A. R. Molecular dynamics simulation of the effect of pH on the adsorption of rhodamine laser dyes on TiO2 hydroxylated surfaces. *Mol. Simul.* **2009**, *35*, 1140−1151.
(48) Zheng, T.; Wu, C.; Chen, M.; Zhang, Y.; Cummings, P. T. Molecular mechanics of the cooperative adsorption of a Pro-Hyp-Gly tripeptide on a hydroxylated rutile TiO2(110) surface mediated by calcium ions. *Phys. Chem. Chem. Phys.* **2016**, *18*, 19757−19764.
(49) Zheng, T.; Zhang, Y.; Wu, C.; Zhou, L.; Cummings, P. T. Molecular investigations of tripeptide adsorption onto TiO2 surfaces: Synergetic effects of surface nanostructure, hydroxylation and bioactive ions. *Appl. Surf. Sci.* **2020**, *512*, 145713.
(50) Serro, A. P.; Fernandes, A. C.; Saramago, B.; Lima, J.; Barbosa, M. A. Apatite deposition on titanium surfaces - The role of albumin adsorption. *Biomaterials* **1997**, *18*, 963−968.
(51) Vlasova, N. N.; Golovkova, L. P. The adsorption of amino acids on the surface of highly dispersed silica. *Colloid J.* **2004**, *66*, 657−662.
(52) Gao, Q.; Xu, W.; Xu, Y.; Wu, D.; Sun, Y.; Deng, F.; Shen, W. Amino acid adsorption on mesoporous materials: Influence of types of amino acids, modification of mesoporous materials, and solution conditions. *J. Phys. Chem. B* **2008**, *112*, 2261−2267.
(53) Meng, M.; Stievano, L.; Lambert, J. F. Adsorption and thermal condensation mechanisms of amino acids on oxide supports. 1. Glycine on silica. *Langmuir* **2004**, *20*, 914−923.
(54) Arteaga, A.; Qu, J.; Haynes, S.; Webb, B. G.; LaFontaine, J.; Rodrigues, D. C. Diabetes as a Risk Factor for Orthopedic Implant Surface Performance: A Retrieval and In Vitro Study. *J. Bio. Tribo. Corros.* **2021**, *7*, 51.
(55) Bourikas, K.; Kordulis, C.; Lycourghiotis, A. Titanium dioxide (Anatase and Rutile): Surface chemistry, liquid-solid interface chemistry, and scientific synthesis of supported catalysts. *Chem. Rev.* **2014**, *114*, 9754−9823.
(56) Brandt, E. G.; Lyubartsev, A. P. Molecular Dynamics Simulations of Adsorption of Amino Acid Side Chain Analogues and a Titanium Binding Peptide on the TiO2 (100) Surface. *J. Phys. Chem. C* **2015**, *119*, 18126−18139.
(57) Kříž, Z.; Klusák, J.; Krištofíková, Z.; Koča, J. How Ionic Strength Affects the Conformational Behavior of Human and Rat Beta Amyloids − A Computational Study. *PLoS One* **2013**, *8*, e62914.
(58) Ibragimova, G. T.; Wade, R. C. Importance of Explicit Salt Ions for Protein Stability in Molecular Dynamics Simulation. *Biophys. J.* **1998**, *74*, 2906−2911.
(59) Kam, H. C.; Ranathunga, D. T. S.; Payne, E. R.; Smaldone, R. A.; Nielsen, S. O.; Dodani, S. C. Spectroscopic characterization and in silico modelling of polyvinylpyrrolidone as an anion-responsive fluorescent polymer in aqueous media. *Supramol. Chem.* **2019**, *31*, 514−522.
(60) Kuhn, B. L.; Osmari, B. F.; Heinen, T. M.; Bonacorso, H. G.; Zanatta, N.; Nielsen, S. O.; Ranathunga, D. T.; Villetti, M. A.; Frizzo, C. P. Dicationic imidazolium-based dicarboxylate ionic liquids: Thermophysical properties and solubility. *J. Mol. Liq.* **2020**, *308*, 112983.
(61) Phillips, J. C.; Braun, R.; Wang, W.; Gumbart, J.; Tajkhorshid, E.; Villa, E.; Chipot, C.; Skeel, R. D.; Kalé, L.; Schulten, K. Scalable molecular dynamics with NAMD. *J. Comput. Chem.* **2005**, *26*, 1781−1802.
(62) Humphrey, W.; Dalke, A.; Schulten, K. VMD: Visual molecular dynamics. *J. Mol. Graphics* **1996**, *14*, 33−38.
(63) Ranathunga, D. T. S.; Shamir, A.; Dai, X.; Nielsen, S. O. Molecular Dynamics Simulations of Water Condensation on Surfaces with Tunable Wettability. *Langmuir* **2020**, *36*, 7383−7391.
(64) Foote, J.; Raman, A. A relation between the principal axes of inertia and ligand binding. *Proc. Natl. Acad. Sci. U. S. A.* **2000**, *97*, 978−983.
(65) Harrison, E. T.; Weidner, T.; Castner, D. G.; Interlandi, G. Predicting the orientation of protein G B1 on hydrophobic surfaces using Monte Carlo simulations. *Biointerphases* **2017**, *12*, 02D401.
(66) Felder, C. E.; Prilusky, J.; Silman, I.; Sussman, J. L. A server and database for dipole moments of proteins. *Nucleic Acids Res.* **2007**, *35*, W512−W521.
(67) Carravetta, V.; Monti, S. Peptide-TiO2 surface interaction in solution by AB initio and molecular dynamics simulations. *J. Phys. Chem. B* **2006**, *110*, 6160−6169.
(68) Köppen, S.; Langel, W. Adsorption of small organic molecules on anatase and rutile surfaces: a theoretical study. *Phys. Chem. Chem. Phys.* **2008**, *10*, 1907.
(69) Monti, S.; Carravetta, V.; Battocchio, C.; Iucci, G.; Polzonetti, G. Peptide/TiO2 surface interaction: A theoretical and experimental study on the structure of adsorbed ALA-GLU and ALA-LYS. *Langmuir* **2008**, *24*, 3205−3214.
(70) Sano, K.-I.; Shiba, K. A Hexapeptide Motif that Electrostatically Binds to the Surface of Titanium. *J. Am. Chem. Soc.* **2003**, *125*, 14234−14235.
(71) Wang, C.; Lu, H.; Wang, Z.; Xiu, P.; Zhou, B.; Zuo, G.; Wan, R.; Hu, J.; Fang, H. Stable liquid water droplet on a water monolayer

https://doi.org/10.1021/acs.langmuir.1c01444
Langmuir XXXX, XXX, XXX−XXX

formed at room temperature on ionic model substrates. *Phys. Rev. Lett.* **2009**, *103*, 137801.
(72) Sampath, J.; Kullman, A.; Gebhart, R.; Drobny, G.; Pfaendtner, J. Molecular recognition and specificity of biomolecules to titanium dioxide from molecular dynamics simulations. *npj Comput. Mater.* **2020**, *6*, 34.
(73) Předota, M.; Zhang, Z.; Fenter, P.; Wesolowski, D. J.; Cummings, P. T. Electric double layer at the rutile (110) surface. 2. Adsorption of ions from molecular dynamics and X-ray experiments. *J. Phys. Chem. B* **2004**, *108*, 12061−12072.
(74) Arima, Y.; Iwata, H. Effect of wettability and surface functional groups on protein adsorption and cell adhesion using well-defined mixed self-assembled monolayers. *Biomaterials* **2007**, *28*, 3074−3082.

https://doi.org/10.1021/acs.langmuir.1c01444
Langmuir XXXX, XXX, XXX−XXX